Tetraacetatodirhodium(II) complexes with tris(methoxyphenyl)phosphines, their reactivity, structure, and antitumor activity

Florian P. Pruchnik, Radosław Starosta, Zbigniew Ciunik, Adam Opolski, Joanna Wietrzyk, Elżbieta Wojdat, and Danuta Duś

Abstract: Reactions of $[Rh_2(\mu\text{-}OAc)_4(H_2O)_2]$ ($[\mathbf{1}\cdot(H_2O)_2]$) with tris(3-methoxyphenyl)phosphine at 1:1 and 1:2 molar ratios yield, first, the appropriate adducts: $[\mathbf{1}\cdot(H_2O)\{P(C_6H_4\text{-}3\text{-}OMe)_3\}]$ and $[\mathbf{1}\cdot\{P(C_6H_4\text{-}3\text{-}OMe)_3\}_2]$, and then $[Rh_2(\mu\text{-}OAc)_3\{\mu\text{-}(C_6H_3\text{-}3\text{-}OMe)P(C_6H_4\text{-}3\text{-}OMe)_2\}(HOAc)_2]$ ($[\mathbf{2}\cdot(HOAc)_2]$), and $[Rh_2(\mu\text{-}OAc)_2\{\mu\text{-}(C_6H_3\text{-}3\text{-}OMe)P(C_6H_4\text{-}3\text{-}OMe)_2\}_2(HOAc)_2]$ ($[\mathbf{3}\cdot(HOAc)_2]$) complexes, respectively. They have been characterized by spectroscopic methods. The molecular structure of $[\mathbf{3}\cdot(HOAc)(H_2O)]$ has been determined crystallographically. The complexes $[\mathbf{3}\cdot(HOAc)_2]$, $[Rh_2(\mu\text{-}OAc)_3\{\mu\text{-}(C_6H_3\text{-}4\text{-}OMe)P(C_6H_4\text{-}4\text{-}OMe)_2\}(HOAc)_2]$ ($[\mathbf{4}\cdot(HOAc)_2]$), and $[Rh_2(\mu\text{-}OAc)_2\{\mu\text{-}(C_6H_3\text{-}4\text{-}OMe)P(C_6H_4\text{-}4\text{-}OMe)_2\}_2(HOAc)_2]$ ($[\mathbf{5}\cdot(HOAc)_2]$) reversibly react with CO giving mono- and biadducts. Antitumor activity of binuclear rhodium(II) compounds $[\mathbf{3}\cdot(HOAc)_2]$, $[Rh_2(\mu\text{-}OAc)_3\{\mu\text{-}(C_6H_3\text{-}2\text{-}O)P(C_6H_3\text{-}2\text{-}OMe)_2\}(HOAc)]$ ($[\mathbf{6}\cdot($HOAc)]), and $[Rh_2(\mu\text{-}OAc)_3\{\mu\text{-}(C_6H_3\text{-}6\text{-}OMe\text{-}2\text{-}O)P[(C_6H_3\text{-}2,6\text{-}(OMe)_2]_2\}(HOAc)]$ ($[\mathbf{7}\cdot(HOAc)]$) have been investigated in vitro. The most active agent for investigated tumor lines is complex $[\mathbf{6}\cdot(HOAc)]$. It shows higher activity than cisplatin (*cis*-$[PtCl_2(NH_3)_2]$). Antitumor activity decreases in the series: $[\mathbf{6}\cdot(HOAc)] > [\mathbf{7}\cdot(HOAc)] > [\mathbf{3}\cdot(HOAc)_2]$. Activity of all investigated rhodium(II) complexes is higher than that of $[\mathbf{1}\cdot(H_2O)_2]$.

Key words: dirhodium(II) complexes, functionalized phosphines, aryl phosphines, ferrocenylmethylphosphines, adducts with CO, antitumor activity, orthometallation reactions.

Résumé : Les réactions du $[Rh_2(OAc)_4(H_2O)_2]$ ($[\mathbf{1}\cdot(H_2O)_2]$) avec la (3-méthoxyphényl)phosphine, à des rapports molaires de 1:1 et 1:2, conduisent à la formation d'adduits appropriés soit premièrement à $[\mathbf{1}\cdot(H_2O)\{P(C_6H_4\text{-}3\text{-}OMe)_3\}]$ et $[\mathbf{1}\cdot\{P(C_6H_4\text{-}3\text{-}OMe)_3\}_2]$ et ensuite à $[Rh_2(OAc)_3\{(C_6H_3\text{-}3\text{-}OMe)P(C_6H_4\text{-}3\text{-}OMe)_2\}(HOAc)_2]$ ($[\mathbf{2}\cdot(HOAc)_2]$) et $[Rh_2(OAc)_2\{(C_6H_3\text{-}3\text{-}OMe)P(C_6H_4\text{-}3\text{-}OMe)_2\}_2(HOAc)_2]$ ($[\mathbf{3}\cdot(HOAc)_2]$). Ces complexes ont été caractérisés par des méthodes spectroscopiques. La structure moléculaire du complexe $[\mathbf{3}\cdot(HOAc)(H_2O)]$ a été déterminée par cristallographie. Les complexes $[\mathbf{3}\cdot(HOAc)_2]$, $[Rh_2(OAc)_3\{(C_6H_3\text{-}4\text{-}OMe)P(C_6H_4\text{-}4\text{-}OMe)_2\}(HOAc)_2]$ ($[\mathbf{4}\cdot(HOAc)_2]$) et $[Rh_2(OAc)_2\{(C_6H_3\text{-}4\text{-}OMe)P(C_6H_4\text{-}4\text{-}OMe)_2\}_2(HOAc)_2]$ ($[\mathbf{5}\cdot(HOAc)_2]$) réagissent de façon réversible avec le CO pour donner des mono- et des bisadduits. On a évalué l'activité antitumorale in vitro des composés binucléaires de rhodium $[\mathbf{3}\cdot(HOAc)_2]$, $[Rh_2(OAc)_3\{(C_6H_3\text{-}2\text{-}O)P(C_6H_3\text{-}2\text{-}OMe)_2\}(HOAc)]$ ($[\mathbf{6}\cdot(HOAc)]$) et $[Rh_2(OAc)_3\{\mu\text{-}(C_6H_3\text{-}6\text{-}OMe\text{-}2\text{-}O)P[(C_6H_3\text{-}2,6\text{-}(OMe)_2]_2\}(HOAc)]$ ($[\mathbf{7}\cdot(HOAc)]$). Le complexe $[\mathbf{6}\cdot(HOAc)]$ est l'agent le plus actif pour les familles de tumeur étudiées. Il présente une activité supérieure à celle du cisplatine, *cis*-$[PtCl_2(NH_3)_2]$. L'activité antitumorale diminue dans la série $[\mathbf{6}\cdot(HOAc)] > [\mathbf{7}\cdot(HOAc)] > [\mathbf{3}\cdot(HOAc)_2]$. L'activité de chacun des complexes de rhodium(II) est supérieure à celle du $[\mathbf{1}\cdot(H_2O)_2]$.

Mots clés : complexes dirhodium(II), phosphines fonctionnalisées, arylphosphines, ferrocénylméthylphosphines, adduits avec le CO, activité antitumorale, réactions d'organométallation.

Introduction

The product of reaction of rhodium tetraacetate with triphenylphosphine, first reported by Cotton and co-workers (1) was one of the first examples of bimetallic *ortho*-metallated compounds. Since that time, attention has been paid to different *ortho*-metallated dirhodium(II) compounds with triaryl and alkyl–aryl phosphines because of the growing interest in the problem of activation of the C—H bond (2–14). However, reactions of tetraacetatodirhodium(II) with

Received September 12, 2000. Published on the NRC Research Press Web site at http://canjchem.nrc.ca on July 3, 2001.

This article is dedicated to Professor Brian R. James on his 65th birthday.

F.P. Pruchnik,[1] R. Starosta, and Z. Ciunik. Faculty of Chemistry, University of Wrocław, 14 F. Joliot-Curie Street, 50-383 Wrocław, Poland.
A. Opolski, J. Wietrzyk, E. Wojdat, and D. Duś. Institute of Immunology and Experimental Therapy, Polish Academy of Sciences, Wrocław, Poland.

[1]Corresponding author (telephone/fax: (+ 48 71) 32 04 232; e-mail: pruchnik@wchuwr.chem.uni.wroc.pl).

 DOI: 10.1139/cjc-79-5/6-868

Table 1. ^{31}P and ^{13}C NMR dirhodium(II) complexes (in $CDCl_3$, room temperature, broadened signal (*), signal from a metallated phenyl ring (^{m})).

Compound	^{31}P NMR: d (ppm), *J* (Hz)	^{13}C NMR: d (ppm), *J* (Hz)
MMP	–2.95 (s)	
[**1**·(H_2O)(MMP)]	–30.2 (dd), ^1J (P-Rh) = 97.7, ^2J (P-Rh) = 31.7	
[**1**·$(MMP)_2$]	–11.0 (s*)	
[**2**·$(HOAc)_2$]	25.0 (dd), ^1J (P-Rh) = 151.4, ^2J (P-Rh) = 4.9	
[**3**·$(HOAc)_2$]	22.6 (d*), ^1J (P-Rh) = 166.8	181.5 (s) (COO bridges); 179.5 (s) (COOH HOAc); $C6^m$: 158.4 (dd) ^1J (Rh-$C2^m$) = 33.3, ^2J (P-$C6^m$) = 12.7; 110–156 (aromatic carbon atoms); 55.33 (s), 54.7 (s), 55.3 (s), and 55.2 (s) (OMe groups); 22.8 (s) (CH_3 bridges); 22.4 (s), 22.3 (s) (CH_3–HOAc)
[**1**·(dhfmp)]	–43.2 (dd), ^1J (P-Rh) = 99.7, ^2J (P-Rh) = 22.4	
[**1**·(hfmp)]	–41.9 (dd), ^1J (P-Rh) = 101.5, ^2J (P-Rh) = 28.2	
[**7**·(hfmp)]	P_A: (dd) 10.66, ^1J (P_A-Rh_A) = 169.1, ^3J (P_A-P_B) = 6.4; P_B: (ddd) –41.34, ^1J (P_B-Rh_B) = 97.3, ^2J (P_B – Rh_A) = 27.3	
[**3**·(HOAc)(hfmp)]	P_A: (dd) 27.64, ^1J (P_A-Rh_A) = 183.1, ^2J (P_A-P_C) = 15.2; P_B: (d) 20.85, ^1J (P_B-Rh_B) = 155.1; P_C: (m) –37	
[**3**·$(hfmp)_2$]	P_A: (d) 24.24, ^1J (P_A-Rh) = 170.4; P_B: (t) –20.52, ^1J (P_B-Rh) = ^2J(P_B-Rh) = 49.6	

functionalized phosphines were not intensively studied. Water-soluble *ortho*-metallated complexes with tris(3-sodium sulfonatophenyl)phosphine (TPPTS), $[Rh_2(\mu\text{-}OAc)_3\{\mu\text{-}(C_6H_3\text{-}3\text{-}SO_3Na)P(C_6H_4\text{-}3\text{-}SO_3Na)_2\}]$, and $[Rh_2(\mu\text{-}OAc)_2\{\mu\text{-}(C_6H_3\text{-}3\text{-}SO_3Na)P(C_6H_4\text{-}3\text{-}SO_3Na)_2\}_2]$ have been investigated (15). It has been found that in reaction of tris(2,4,6-trimethoxyphenyl)phosphine (TMPP) (16–18), tris(2-methoxyphenyl)phosphine (OMP) (19, 20), and tris(2,6-dimethoxyphenyl)phosphine (DOMP) (20) with [**1**·$(H_2O)_2$], the O—CH_3 bond is split off and complexes with Rh-$P(C_6H_3(R)OMe)_2C_6H_2(R)(R')O$-Rh (where R, R′ = H or OMe) bridges are formed. In this paper we report on synthesis of $[Rh_2(\mu\text{-}OAc)_3\{\mu\text{-}(C_6H_3\text{-}3\text{-}OMe)P(C_6H_4\text{-}3\text{-}OMe)_2\}(HOAc)_2]$ ([**2**·$(HOAc)_2$]) and $[Rh_2(\mu\text{-}OAc)_2\{\mu\text{-}(C_6H_3\text{-}3\text{-}OMe)P(C_6H_4\text{-}3\text{-}OMe)_2\}_2(HOAc)_2]$ ([**3**·$(HOAc)_2$]) as well as properties and reactivity of binuclear rhodium(II) complexes containing other *ortho-C*- and *ortho-O*-metallated tris(methoxyphenyl)phosphines.

It has been known for many years, that rhodium(II) carboxylato complexes $[Rh_2(\mu\text{-}O_2CR)_4]$ and their derivatives (21–25), complexes $[Rh_2(\mu\text{-}O_2CR)_2(\mu\text{-}N\text{-}N)_2(H_2O)_2]^{2+}$ (N-N = bpy, phen) (25–31) are promising antitumor agents. However, antitumor properties of rhodium(II) complexes with phosphine bridges were not examined. Here we describe antitumor activity in vitro of some binuclear rhodium(II) compounds with methoxyphenylphosphines, namely complexes [**3**·$(HOAc)_2$], $[Rh_2(\mu\text{-}OAc)_3\{\mu\text{-}(C_6H_4\text{-}2\text{-}O)P(C_6H_4\text{-}2\text{-}OMe)_2\}(HOAc)]$ ([**6**·(HOAc)]) and $[Rh_2(\mu\text{-}OAc)_3\{\mu\text{-}(C_6H_3\text{-}6\text{-}OMe\text{-}2\text{-}O)P[(C_6H_3\text{-}2,6\text{-}(OMe)_2]_2\}(HOAc)]$ ([**7**·(HOAc)]), dhfmp as well as, for comparison, activity of *cis*-diaminadichloroplatinum(II).

Results and discussion

Syntheses of Rh(II) complexes with methoxyphenylphosphines

In reactions of [**1**·$(L)_2$] (L = Lewis base) and other dirhodium(II) carboxylates with phosphines, PR_3 ligands are first coordinated along the Rh-Rh axis forming reactive adducts [**1**·(PR_3)L] or [**1**·$(PR_3)_2$].

Formation of mono- and biadducts of [**1**·$(H_2O)_2$] with MMP ([**1**·(H$_2$O)(MMP)] and [**1**·$(MMP)_2$]) was followed with ^{31}P NMR spectroscopy. For the monoadduct in $CDCl_3$, a doublet of doublets at –30.2 ppm (^1J (P-Rh) = 97.7 Hz, ^2J (P-Rh) = 31.7 Hz) and for the biadduct, a broad singlet at –11.0 ppm have been observed (see Table 1). This indicates that axial phosphine ligands in the biadduct are labile. Coordination chemical shifts ($\Delta\delta$ (^{31}P) = δ (P_{adduct}) – δ (P_{ligand})) are –27.25 and –8.05 ppm for monoadduct and biadduct, respectively. $\Delta\delta$ (^{31}P) values are similar to those found in analogous dirhodium(II) compounds with other phosphines: ca. –30 and –10 ppm for monoadducts and biadducts, respectively, (2–4, 6–10, 12, 15, 18, 20, 32). Analogous adducts [**1**·(PR_3)] and [**1**·$(PR_3)_2$] were obtained with TPPTS (15) and PMP (21).

In the next step, phosphine ligands migrate to equatorial coordination sites and then the C—H bond of the PR_3 ligand can be activated giving the binuclear product of *ortho*-metallation.

In the reaction of [**1**·$(H_2O)_2$] with MMP complexes, $[Rh_2(\mu\text{-}OAc)_3\{\mu\text{-}(C_6H_3\text{-}3\text{-}OMe)P(C_6H_4\text{-}3\text{-}OMe)_2\}(HOAc)_2]$ ([**2**·$(HOAc)_2$]) and mainly [**3**·$(HOAc)_2$] were obtained.

In the contrast to the selective reactions of tris(4-methoxyphenyl)phosphine (PMP) with rhodium(II) acetate, which give $[Rh_2(\mu\text{-}OAc)_3\{\mu\text{-}(C_6H_3\text{-}4\text{-}OMe)P(C_6H_4\text{-}4\text{-}OMe)_2\}(HOAc)_2]$ ([**4**·$(HOAc)_2$]) and $[Rh_2(\mu\text{-}OAc)_2\{\mu\text{-}(C_6H_3\text{-}4\text{-}OMe)P(C_6H_4\text{-}4\text{-}OMe)_2\}_2(HOAc)_2]$ ([**5**·$(HOAc)_2$]) complexes at [**1**·$(H_2O)_2$]:PMP ratios equal to 1:1 and 1:2, respectively, (32), in the reactions of MMP with [**1**·$(H_2O)_2$] we obtained mainly [**3**·$(HOAc)_2$]. A mixture of compounds [**3**·$(HOAc)_2$], [**2**·$(HOAc)_2$], and [**1**·$(H_2O)_2$] was obtained even in the presence of excess of rhodium(II) acetate, at ratios of [**1**·$(H_2O)_2$]:MMP > 1. Thus complex [**2**·$(HOAc)_2$] is very reactive and can be easily transformed into compound [**3**·$(HOAc)_2$].

In the case of reactions of [**1**·$(H_2O)_2$] with methoxyphenylphosphines containing methoxy groups in *ortho* posi-

Table 2. ^{1}H NMR dirhodium(II) complexes (in $CDCl_3$, room temperature, broadened signal (*), signal from a metallated phenyl ring ($^{(m)}$)).

Compound	^{1}H NMR: d (ppm), *J* (Hz)
MMP	3.71 (s, 9H) (OMe groups); 6.8–7.3 (aromatic protons)
[**1**·(H_2O)(MMP)]	3.67 (s, 9H) (OMe groups); 1.73 (s*, 9H) (OAc bridges); 6.9–7.4 (aromatic protons)
[**1**·$(MMP)_2$]	3.66 (s, 18H^{OMe}) (OMe groups); 1.59 (s, 12H) (OAc bridges); 6.9–7.4 (aromatic protons)
[**2**·$(HOAc)_2$]	1.30 (s, 6H) (OAc bridges, *cis*); 2.32 (s, 3H) (OAc bridge, *trans*); 2.20 (s, 6H) (axial molecules of HOAc); 3.68 (s, 6H) (OMe groups); 3.65 (s, 3H) (OMe group$^{(m)}$); 6.5–8.5 (aromatic protons)
[**3**·$(HOAc)_2$]	1.20 (s, 6H) (OAc bridges); 2.14 (s, 6H) (axial molecules of HOAc); 3.43 (s, 6H) (OMe groups); 3.51 (s, 6H) (OMe groups); 3.76 (s, 6H) (OMe groups$^{(m)}$); 6.2–7.4 (aromatic protons)
[**1**·(dhfmp)]	1.84 (s) (OAc bridges); 2.0–4.4 (ligand's protons)
[**1**·(hfmp)]	1.87 (s) (OAc bridges); 2.0–4.5 (ligand's protons)
[**7**·(hfmp)]	1.25 (s, 3H) (OAc bridge); 1.27 (s, 3H) (OAc bridge); 1.72 (s, 3H) (OAc bridge); 2.08 (s, 3H) (molecule of HOAc); 3.14 (s, 3H) (OMe group); 3.30 (s, 3H) (OMe group); 3.33 (s, 3H) (OMe group); 3.40 (s, 3H) (OMe group); 4.09 (s, 10H^A) (cyclopentadienyl ring); 4.65 (s, 3H) (OMe group); 2.5–4.5 (other protons of hfmp) 6.11 (dd) ^3J (H-H) = 7.92, ^4J (H-P) = 4.20; 6.13 (dd) ^3J (H-H) = 7.92, ^4J (H-P) = 4.68; 6.34 (dd) ^3J (H-H) = 8.14, ^4J (H-P) = 3.49; 6.41 (dd) ^3J (H-H) = 8.15, ^4J (H-P) = 1.65; 6.50 (dd) ^3J (H-H) = 7.68, ^4J (H-P) = 4.89; 6.88 (dd) ^3J (H-H) = 8.16, ^4J (H-P) = 4.89; 6.95 (t) ^3J (H-H) ≈ ^4J (H-P) = 8.16; 7.02 (t) ^3J (H-H) ≈ ^4J (H-P) = 8.14; 7.35 (t) ^3J (H-H) ≈ ^4J (H-P) = 8.14
[**3**·(HOAc)(hfmp)]	1.14 (s, 3H) (OAc bridge); 1.12 (s, 3H) (OAc bridge); 2.07 (s, 6H) (molecule of HOAc); 4.13 (s, 10H^A) (cyclopentadienyl ring); 2.6–5.5 (OMe groups and protons of hfmp); 5.8–7.5 (aromatic protons)
[**3**·$(hfmp)_2$]	1.00 (s, 6H) (OAc bridges); 2.07 (s, 6H) (molecule of HOAc); 4.15 (s, 10H^A) (cyclopentadienyl ring); 2.6–5.5 (OMe groups and protons of hfmp); 5.8–7.5 (aromatic protons)

tions, the O—Me bond of the methoxy group is activated and a Rh-PC_6H_2RR'–2-O-Rh bridge is formed. Thus, tris(2-methoxyphenyl)phosphine (OMP) and tris(2,6-dimethoxyphenyl)phosphine (DOMP), at molar ratio [P]:[Rh_2] of 2:1, give complexes [**6**·(HOAc)] (19, 20) and [**7**·(HOAc)] (20) with only one bridging phosphine ligand. In these reactions, a methyl cation of one of the methoxy groups is split off and a $\{(CH_3)PAr_3\}^+$ cation is formed.

Complexes [**2**·$(HOAc)_2$] and [**3**·$(HOAc)_2$] have been characterized by a combination of ^{1}H, ^{13}C, and ^{31}P NMR spectroscopies (Table 2). The Chemical shift of OAc groups in *cis* positions is much lower (1.30 ppm, 6H) than that for the OAc bridge (2.32 ppm, 3H) in the *trans* position relative to the phosphine bridging ligand coordinated via P and C (*ortho*) atoms. Both coordination chemical shift and Rh-P coupling constants (^1J (P-Rh) = 151.4 Hz, ^2J (P-Rh) = 4.9 Hz) for complex [**2**·$(HOAc)_2$] (Table 2) are typical of *ortho*-metallated complexes [$Rh_2(\mu\text{-}OAc)_3\{\mu\text{-}(C_6H_3R)P(C_6H_4R)_2\}$]. In the case of complex [**4**·$(HOAc)_2$], ^1J (P-Rh) = 147.4 Hz and ^2J (P-Rh) = 6.1 Hz (22). The ^{1}H, ^{13}C, and ^{31}P NMR data indicate that complex [**3**·$(HOAc)_2$] has a head-to-tail structure. The ^1J (P-Rh) = 166.8 Hz for compound [**3**·$(HOAc)_2$] and is similar to that found for complex [**5**·$(HOAc)_2$] (168.9 Hz).

Molecular structure of [3·(H_2O)(HOAc)]

The molecular structure of [**3**·(H_2O)(HOAc)] shown in Fig. 1 confirms the structure of [**3**·$(HOAc)_2$] established with spectroscopic methods. Details of X-ray data collected are summarized in Table 3. Table 4 contains selected bond lengths and angles. The structure consists of a binuclear rhodium core bridged by two acetate groups and two MMP ligands in which *ortho*-metallation has occurred at one of the phenyl rings. The bridging phenyl rings are coordinated via C-6 atoms: C(46) and C(16). Phosphine ligands are in *cis* position to each other with H-T (head-to-tail) structure. One of the axial sites is occupied by a molecule of water and the second one by a molecule of acetic acid.

The molecular structure shows distorted octahedral coordination around the central atoms. The complex has an almost eclipsed conformation, torsion angles O(1)-Rh(1)-Rh(2)-O(2) and O(3)-Rh(1)-Rh(2)-O(4) are 19.4° and 17.6°, respectively. The torsion angles of the bridging *ortho*-metallated ligand are slightly smaller: P(1)-Rh(1)-Rh(2)-C(16) = 14.2° and P(2)-Rh(2)-Rh(1)-C(46) = 13.8°. The Rh(1)—Rh(2) distance is 2.4913(18) Å, indicating a rather strong single bond between two metal atoms. Rh(1)—P(1) and Rh(2)—P(2) bond lengths are 2.193 Å and Rh(1)—C(46) and Rh(2)—C(16) distances are 1.993(14) and 1.995(14) Å, respectively. Lengths of Rh—O^{equatorial} bonds change in the range 2.12–2.17 Å. The bond lengths between the phosphorus atom and carbon atom of the metallated ring are shorter than those between the phosphorus and carbon atoms of the nonmetallated rings. Methoxy substituents in the phosphine ligands lie approximately in the planes of the phenyl rings.

Lengths of rhodium – axial ligand bonds (Rh(1)—O(1w) = 2.313(9) Å, Rh(1)—O(5) = 2.363(12) Å) indicate rather weak bonding of these ligands. HOAc molecule is coordinating via oxygen atom of carbonyl group; the -OH group is involved in the formation of a strong hydrogen bond with the oxygen atom of the bridging acetato ligand (O(6)-H(6)···O(2), d_{O-O} = 2.565(18) Å).

A rather strong intermolecular hydrogen bond is formed between the axial molecule of water and the oxygen atom of the acetate bridge of another molecule of the compound (O(1w)-H(2w)···O(3) (1 –*x*, 2 – *y*, –*z*), d_{O-O} = 2.695(13) Å).

Reactions of *ortho*-metallated complexes

Complex [**3**·$(HOAc)_2$], as other dirhodium(II) carboxylates and their derivatives, reacts with ligands showing σ-donor and π-acceptor properties as well as with ligands

Fig. 1. Molecular structure of [**3**·(H_2O)(HOAc)] (an OTREP (49) drawing with 30% thermal ellipsoids).

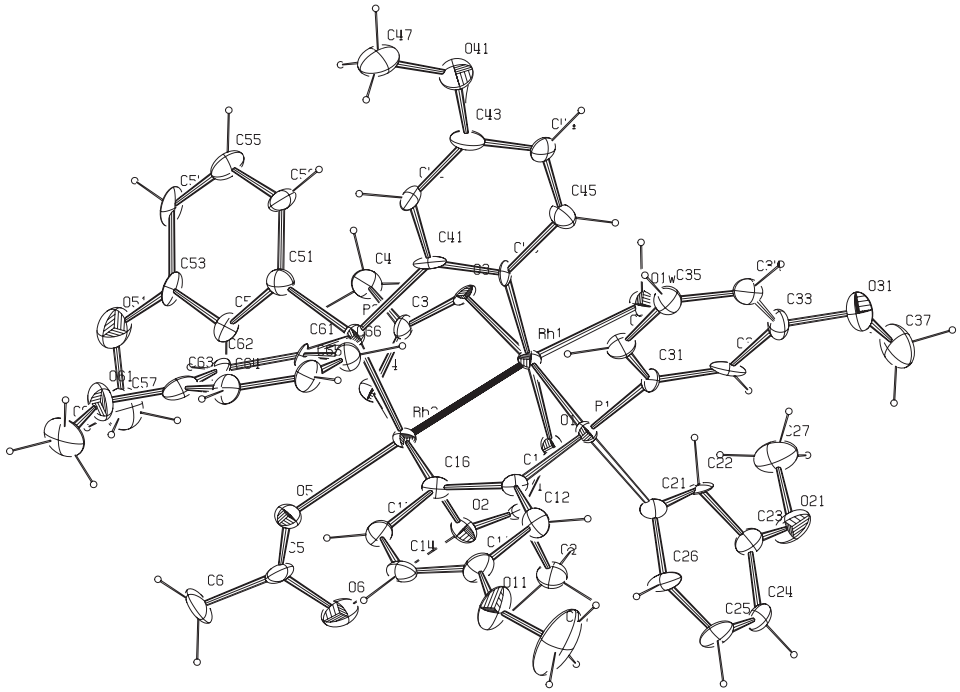

Table 3. Crystal data and details of the structure determination for [**3**·(H_2O)(HOAc)].

Empirical formula	$C_{48}H_{52}O_{13}P_2Rh_2$
Formula weight	1104.66
T (K)	170(2)
λ (Å)	0.71073
Crystal system	Triclinic
Space group	$P\bar{1}$
a (Å)	11.026(2)
b (Å)	15.290(3)
c (Å)	15.653(3)
α (°)	71.34(3)
β (°)	69.53(3)
γ (°)	75.69(3)
V (Å^3)	2314.9(10)
Z	2
D_c (mg m^{-3})	1.585
μ (mm^{-1})	0.8
F(000)	1128
Crystal size (mm)	0.1 × 0.05 × 0.02
Diffractometer	Kuma KM4CCD
θ range for data collection (°)	2.6–22.5
Index ranges	*h*:→ –11:11; *k*:→ –16:15; *l*:→ –16:16
Reflections collected	10 938
Independent reflections	5941
Data (parameters)	591
Weighting scheme: *a*, *b*, *c*[a]	0.00, 29.39, 3.00
Goodness-of-fit (F^2)	1.19
Final R_1 and wR_2 indices ($I > 2\sigma I$)	0.0973, 0.1907
Largest diff. peak and hole (e Å^{-3})	–0.72, 0.80

[a] $w = 1/[\sigma^2(F_o^2) + (a \times P)^2 + b \times P]$ where $P = [\max(F_o^2, 0) + 2 \times F_c^2]/c$.

possessing only σ-donor properties. Adducts [**3**·(L)] and [**3**·$(L)_2$] are the products of these reactions.

Reactions of complex [**3**·$(HOAc)_2$] with {(η^5-C_5H_5)Fe(η^5-C_5H_4)CH_2}$_2$$PCH_2OH$ (hfmp) (Table 2) give stable complexes. Pure adducts [**3**·(hfmp)(HOAc)] and [**3**·$(hfmp)_2$] can be obtained in chloroform at a [**3**·$(HOAc)_2$]:hfmp ratio equal to 1:1 and 1:2, respectively. However, $\Delta\delta$ (^{31}P) = δ (P_{adduct}) – δ (P_{ligand}) for axial hfmp ligands in this case are lower than those for adducts with arylphosphines: –19.1 and –2.6 ppm for [**3**·(hfmp)(HOAc)] and [**3**·$(hfmp)_2$], respectively, (Table 2). Coordination of the ferrocenylmethylphosphine ligand causes large changes in chemical shifts of the bridging MMP ligand; binding hfmp as axial ligand moves the signals of MMP to lower fields and raises the coupling constants between MMP and rhodium atom. In [**3**·(hfmp)(HOAc)], there are two signals of *ortho*-metallated MMP ligand: a doublet of doublets at 27.6 ppm (^1J (P-Rh) = 183.1 Hz, ^2J (P-P) = 15.2 Hz) and a doublet at 20.85 ppm (^1J (P-Rh) = 155.1 Hz); in biadduct [**3**·$(hfmp)_2$] there is only one doublet of MMP at 24.2 ppm (^1J (P-Rh) = 170.4 Hz).

For monoadducts [**1**·(hfmp)(H_2O)], [**1**(dhfmp)$(H_2O)_2$] (dhfmp = (η^5-C_5H_5)Fe(η^5-C_5H_4)$CH_2P(CH_2OH)_2$), and [**7**·(hfmp)], almost the same $\Delta\delta$ (^{31}P) were observed as for [**3**·(HOAc)(hfmp)].

Complex [**3**·$(HOAc)_2$] in methanol, acetone, and chloroform under a CO atmosphere very easily forms biadduct [**3**·$(CO)_2$] that is considerably more stable than adducts [**6**·(CO)], [**6**·$(CO)_2$], and [**7**·(CO)] (20). Complex [**3**·$(CO)_2$] is stable in these solvents in an air, nitrogen, or argon atmosphere at room temperature for several hours. The first band observed in the electronic spectrum of complex [**3**·$(HOAc)_2$] in acetone at 559 nm is shifted to 399 nm in biadduct [**3**·$(CO)_2$]. The spectrum of the starting compound can be observed after prolonged bubbling of nitrogen through solution, which proves reversibility of the binding of CO. The

Table 4. Selected bond lengths and angles in [**3**·(H_2O)(HOAc)].

Bond lengths	(Å)	Angles	(°)
Rh((1)—Rh(2)	2.4913(18)	Rh(2)-Rh(1)-P(1)	88.38(11)
Rh(1)—P(1)	2.193(4)	Rh(2)-Rh(1)-O(1)	83.9(3)
Rh(1)—O(1)	2.188(10)	Rh(2)-Rh(1)-O(1W)	162.3(3)
Rh(1)—O(1W)	2.313(9)	Rh(2)-Rh(1)-O(3)	86.8(3)
Rh(1)—O(3)	2.122(10)	Rh(2)-Rh(1)-C(46)	96.7(4)
Rh(1)—C(46)	1.993(14)	P(1)-Rh(1)-O(1)	94.8(3)
Rh(2)—P(2)	2.193(5)	P(1)-Rh(1)-O(1W)	99.8(3)
Rh(2)—O(2)	2.127(10)	P(1)-Rh(1)-O(3)	175.2(3)
Rh(2)—O(4)	2.177(10)	P(1)-Rh(1)-C(46)	90.5(4)
Rh(2)—O(5)	2.363(12)	O(1W)-Rh(1)-O(3)	84.9(4)
Rh(2)—C(16)	1.995(14)	Rh(1)-Rh(2)-P(2)	88.34(13)
P(1)—C(11)	1.805(13)	Rh(1)-Rh(2)-O(2)	86.0(3)
P(1)—C(21)	1.848(15)	Rh(1)-Rh(2)-O(4)	83.5(3)
P(1)—C(31)	1.813(17)	Rh(1)-Rh(2)-O(5)	163.7(3)
P(2)—C(41)	1.813(17)	Rh(1)-Rh(2)-C(16)	96.5(4)
P(2)—C(51)	1.833(16)	P(2)Rh(2)-O(2)	174.3(3)
P(2)—C(61)	1.824(16)	P(2)-Rh(2)-O(4)	93.1(3)
O(1)—C(1)	1.243(18)	P(2)-Rh(2)-O(5)	101.2(3)
O(2)—C(1)	1.236(19)	P(2)-Rh(2)-C(16)	90.2(4)
O(3)—C(3)	1.268(19)		
O(4)—C(3)	1.244(17)		

Hydrogen bonds: A-H (Å), H···B (Å), A-B (Å), A-H···B (°)
O(1W)-H(2W)···O(3) [1 −*x*, 2 − *y*, −*z*]: 1.0792, 1.7625, 2.695(13), 141.88

O(6)-H(6)···O(2): 0.8203, 1.7809, 2.565(18), 159.30

presence of [**3**·$(CO)_2$] was also demonstrated by the ^{1}H and ^{13}C NMR spectra of complex [**3**·$(HOAc)_2$] in $CDCl_3$ in an atmosphere of ^{13}CO (Tables 5 and 6). The AA′XX′ type spectrum of the ^{13}CO ligand has been observed at 243 K (d = 174.4 ppm, ^1J (C-Rh) = 46.5 Hz, ^2J (C-Rh) = 4.0 Hz, $^3J_{C-C}$ = 31.7 Hz, and ^1J (Rh-Rh) = 3.5 Hz) (Table 6, Fig. 2).

Relatively high stability of the Rh—CO bond in [**3**·$(CO)_2$] was confirmed by IR spectra. Stretching frequency ν (CO) for this adduct is low (2036 cm^{-1}) and similar to ν (CO) observed for [**5**·$(CO)_2$] (2032 cm^{-1}). This band is shifted to 1991 cm^{-1} for complex [**3**·$(^{13}CO)_2$], which agrees very well with the calculated value. For other adducts, the ν (CO) frequencies are higher, e.g., [**1**·$(CO)_2$] (2105 cm^{-1}), [**7**·(CO)] (2084 cm^{-1}), [**6**$(CO)_n$] (2085 and 2105 cm^{-1}).

Adducts [**4**·(CO)(HOAc)] and [**4**·$(CO)_2$] are less stable than [**3**·$(CO)_2$]. They are relatively stable in chloroform solutions and less stable in more polar solvents, methanol and acetone. At room temperature, in chloroform, the mixture of labile monoadduct [**4**·(CO)(HOAc)] and biadduct [**4**·$(CO)_2$] is formed. This was confirmed by ^{31}P and ^{13}C NMR spectra of these complexes in chloroform under CO atmosphere (Table 6). In the ^{31}P NMR spectrum only one doublet was observed at 11.7 ppm (^1J (P-Rh) = 140.2 Hz). This signal is shifted for 3 ppm to higher fields in comparison with complex [**4**·$(HOAc)_2$]. In the ^{13}C NMR spectrum at room temperature, ligand ^{13}CO gave a broad singlet at 165 ppm. However, the ^{31}P and ^{13}C spectra at 243 K indicate that monoadduct [**4**·(CO)(HOAc)] and biadduct [**4**·$(CO)_2$] are rigid. In the ^{31}P NMR spectrum, two doublets of the ratio of intensities 4.5:5.5 are observed. In the ^{13}C NMR spectrum of [**4**·$(^{13}CO)_2$] and [**4**·(^{13}CO)] at 243 K one can observe two broad singlets at 171.6 and 168.8 ppm which can be assigned to [**4**·$(CO)_2$] and a broad doublet at 156.1 ppm (^1J (C-Rh) = 45.8 Hz). Two signals of ^{13}CO in the biadduct are observed due to unequivalent axial positions in complex **4**. The doublet at 156.1 ppm should be assigned to [**4**·(CO)]. Similar chemical shift and ^1J (C-Rh) were found for monoadduct [**7**·(^{13}CO)] (δ (^{13}C) = 153 ppm, ^1J (P-Rh) = 42.0 Hz) (20). The approximate [**4**·(CO)(HOAc)]:[**4**·$(CO)_2$] ratio calculated from ^{13}C NMR is 3:7 and is similar to that determined from the ^{31}P NMR spectrum.

Antitumor activities of investigated complexes

We have investigated antitumor activity in vitro of some complexes against a few cell lines (KB (oral carcinoma), Hu1703 (bladder cancer), SW707 (colon adenocarcinoma), and T47D (breast cancer). Activities of investigated compounds [**3**·$(HOAc)_2$], [**6**·(HOAc)], [**7**(HOAc)], and dhfmp were compared to the activity of *cis*-diaminadichloroplatinum(II) (Table 7).

The most active agent against all investigated tumor lines is complex [**6**·(HOAc)]. It shows higher activity than cisplatin. Antitumor activity decreases in the series: [**6**·(HOAc)] > [**7**·(HOAc)] > [**3**·$(HOAc)_2$] > dhfmp. Activity of all investigated rhodium(II) complexes is higher than that of [**1**·$(H_2O)_2$].

To explain possible mechanisms of antitumor activity of these complexes we have investigated interactions in situ of complexes [**3**·$(HOAc)_2$] and [**6**·(HOAc)] with adenine, adenosine, AMP, ATP, guanine, guanosine, cytosine, cytidine, glutathione (GSH), oxidized glutathione (GSSG), and cysteine using UV–vis spectroscopy. Complex [**6**·(HOAc)] reacts immediately with adenine, adenosine, AMP, and ATP giving adducts most probably coordinated with the Rh atom via the N7 atom. This follows from the blue shift of the first band in the visible region from 618 nm for compound **5** to 564 nm for the adduct with adenine and 566 nm for the one with adenosine. The lowest shift, to 596 nm, was observed in the case of the adduct with ATP (Fig. 3). This observation is supported by literature data indicating that adenine and adenosine, when coordinated as axial ligands to dirhodium(II) complexes, usually interact via the N7 atom (33–35). Spectra of a solution containing [**6**·(HOAc)] and 10-fold excess of guanine, guanosine, cytidine, or cytosine are very similar to the spectrum of the pure complex. Thus, these nucleotide bases do not interact with complex [**6**·(HOAc)] or are coordinated through the O atom and therefore can be easily substituted by other oxygen-containing ligands present in cells (H_2O, $RCOO^-$, etc.). Interaction of adenine with complex [**3**·$(HOAc)_2$] is much weaker than with compound [**6**·(HOAc)]. The first band observed at 547 nm was shifted only to 545 nm after addition of 10 mol of adenine.

Complex [**6**·(HOAc)] easily reacts with compounds containing sulfhydryl groups, GSH, and cysteine. Even at a molar ratio [**6**·(HOAc)]:HSR of 1:1, the complex immediately is reduced to the diamagnetic mixed valence Rh(I)–Rh(II) complexes, most likely containing a Rh_4^{6+} core, showing a very intensive band at 552 nm (Fig. 4). It was found that complexes $[Rh_2(\mu\text{-}OAc)_2(\mu\text{-}N\text{-}N)_2(H_2O)_2]^{2+}$ can also be readily reduced with sulfhydryl compounds (GSH, cysteine,

Table 5. ^{1}H NMR spectra of [**3**·(HOAc)$_2$] and [**4**·(HOAc)$_2$] complexes with CO (broadened signal (*), signal from a metallated phenyl ring (^{m})).

Compound	^{1}H NMR: d (ppm), *J* (Hz)
[**4**·(HOAc)$_2$] + CO (MeOH-d_4, room temperature)	1.27 (s, 6H) (*cis* OAc bridges); 2.17 (s, 3H) (*trans* OAc bridge), 1.98 (s, 6H) (molecules of HOAc); 3.80 (s, 6H) (OMe groups), 3.84 (s, 3H) (OMe group$^{(m)}$); H2.6: 7.34 (dd, 4H), ^{3}J (H2.6-P) = 10.3, ^{3}J (H2.6- H3.5) = 8.9; H3.5: 6.93 (dd, 4H), ^{4}J (H3.5- P) = 1.8; H3^{m}: hidden under H2.6; H5^{m}: 6.46 (dt, 1H), ^{3}J (H5^{m}-H6^{m,}) = 8.5, ^{4}J(H5^{m}-P) ≈ ^{4}J(H5^{m}-H3^{m}) = 2.0; H6^{m}: 6.70 (dd, 1H), ^{3}J(H6^{m}-P) = 10.3
[**4**·(HOAc)$_2$] + ^{13}CO ($CDCl_3$, room temperature)	1.33 (s, 6H) (OAc bridges, *cis*); 2.25 (s, 3H) (OAc bridge, *trans*); 2.09 (s, 6H) (molecules of HOAc); 3.77 (s, 6H) (OMe groups); 3.86 (s, 3H) (OMe group$^{(m)}$); H2.6: 7.29 (dd, 4H), ^{3}J (H$^{2.6}$-P) = 10.8, ^{3}J (H2.6- H3.5) = 8.8; H3.5: 6.84 (dd, 4H), ^{4}J(H3.5- P) = 2.0; H3^{m}: 7.47 (s*, 1H); H5^{m}: 6.46 (dt, 1H), ^{3}J (H5^{m}-H6^{m,}) = 8.4, ^{4}J (H5^{m}-P) ≈ ^{4}J (H5^{m}-H3^{m}) = 2.0; H6^{m}: 6.70 (dd, 1H), ^{3}J (H6^{m}-P) = 10.3
[**4**·(HOAc)$_2$] + ^{13}CO ($CDCl_3$, 243 K)	1.32 (s*, 6H) (OAc bridges, *cis*); 2.27 (s*, 3H) (OAc bridge, *trans*); 2.11 (s*, 6H) (molecules of HOAc); 3.73 (s*, 6H) (OMe groups); 3.83 (s*, 3H) (OMe group$^{(m)}$); 7.4–6.3 (aromatic protons)
[**3**·(HOAc)$_2$] + CO (MeOH-d_4, room temperature)	1.17 (s, 6H) (OAc bridges); 1.98 (s, 6H) (molecules of HOAc); 3.52 (s, 6H) (OMe groups); 3.55 (s, 6H) (OMe groups); 3.78 (s, 6H) (OMe groups); 7.4–6.2 (aromatic protons)
[**3**·(HOAc)$_2$] + CO ($CDCl_3$, room temperature)	1.22 (s, 6H) (OAc bridges); 2.05 (s, 6H) (molecules of HOAc); 3.48 (s, 6H) (OMe groups); 3.51 (s, 6H) (OMe groups); 3.77 (s, 6H) (OMe groups); 7.3–6.2 (aromatic protons)
[**3**·(HOAc)$_2$] + ^{13}CO ($CDCl_3$, 243 K)	1.19 (s, 6H) (OAc bridges); 2.09 (s, 6H) (molecules of HOAc); 3.84 (s, 6H) (OMe groups); 3.51 (s, 6H) (OMe groups); 3.55 (s*, 6H) (OMe groups); 7.5–6.2 (aromatic protons)

Table 6. ^{31}P and ^{13}C NMR spectra of [**3**·(HOAc)$_2$] and [**4**·(HOAc)$_2$] complexes with CO (broadened signal (*), signal from a metallated phenyl ring (^{m})).

Compound	^{31}P NMR	^{13}C NMR
[**4**(HOAc)$_2$] + CO (MeOH-d_4, room temperature)	15.2 (d), ^{1}J (P-Rh) = 143	
[**4**·(HOAc)$_2$] + ^{13}CO ($CDCl_3$, room temperature)	11.7 (d), ^{1}J (P-Rh) = 140.2	
[**4**·(HOAc)$_2$] + ^{13}CO ($CDCl_3$, 243 K)	13.4 (d), ^{1}J (P-Rh) = 149.2 (55%); 11.7 (d), ^{1}J (P-Rh) = 124.3 (45%)	^{13}CO: 171.6 (s*), 168.8 (s*), 156.1 (d*) 45.8
[**3**·(HOAc)$_2$] + CO (MeOH-d_4, room temperature)	15.1 (d), ^{1}J (P-Rh) = 152.6	
[**3**·(HOAc)$_2$] + CO ($CDCl_3$, room temp.)	13.2 (d), ^{1}J (P-Rh) = 151.5	
[**3**·(HOAc)$_2$] + ^{13}CO ($CDCl_3$, 243 K)	14.2 (d), ^{1}J (P-Rh) = 149.0	^{13}CO: (AA′ part of AA′XX′): 174.38 ppm, ^{3}J (^{13}C–^{13}C) = 31.7, ^{1}J (Rh-Rh) = 3.5, ^{1}J (^{13}C-Rh) = 46.5, ^{2}J (^{13}C-Rh) = 4.0

and coenzyme A) giving polynuclear rhodium compounds (36) intensively absorbing in the same region, at ca. 590 nm. Similar spectra were also observed for tetranuclear and polynuclear complexes with isocyanides $[Rh_4(\mu\text{-}CNRNC)_8]^{6+}$ (37–40), $[Rh_4(OAc)_4(N\text{-}N)_4](OAc)_2$ (41), and $\{[Rh_2(OAc)_2(N\text{-}N)_2]^{+}\}_nX_n^{-}$ (42), where N-N = bpy, phen and $X^{-} = BF_4^{-}$, PF_6^{-}. Interaction of complex [**6**·(HOAc)] with GSSG is very weak and the electronic spectrum of [**6**·(HOAc)] after addition of GSSG almost does not change. That proves that complex [**6**·(HOAc)] is easily reduced with GSH.

Absorbance of the reaction product of complex [**3**·(HOAc)$_2$] with GSH is considerably greater than the starting compound, however in the 750–400 nm region, only a shoulder at ca. 550 nm is present (Fig. 5). This suggests that reduction of compound [**3**·(HOAc)$_2$] with GSH proceeds less effectively than reduction of complex [**6**·(HOAc)].

Antitumor activity of complex [**6**·(HOAc)], reacting effectively with adenine and its derivatives and with sulfhydryl compounds, is much higher than the activity of complex [**3**·(HOAc)$_2$] that reacts with the same compounds much less intensely.

Fig. 2. Fragment of the ^{13}C NMR spectrum of [**3**·($^{13}CO)_2$] spectrum in $CDCl_3$ (temperature 243 K) (^{13}CO groups signal (AA′XX′ type)).

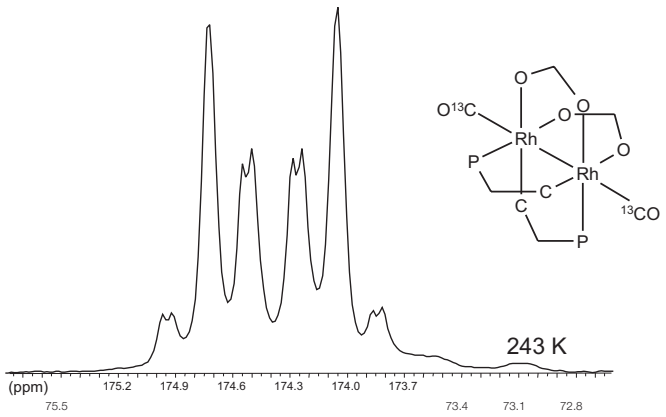

Experimental

Procedures and materials

Tris(4-methoxyphenyl)phosphine (PMP), tris(3-methoxyphenyl)phosphine (MMP), tris(2-methoxyphenyl)phosphine (OMP), and tris(2,6-dimethoxyphenyl)phosphine (DOMP) were purchased from Strem or Avocado and used without further purification. Adenine, adenosine, adenosine 5′-monophosphate (AMP), adenosine 5′-triphosphate (ATP), guanine, guanosine, cytosine, cytidine, glutathione (GSH), oxidized glutathione (GSSG), and cysteine were purchased from Reanal (Hungary) and also used as purchased. All solvents were deoxidized prior to use. Infrared spectrum (KBr pellet) was measured on a Bruker IFS 113v and UV–vis spectra on a Beckman DU 7500 spectrometer. ^1H NMR and ^{31}P NMR spectra were measured in $CDCl_3$ on a Bruker AMX 300 spectrometer with traces of $CHCl_3$ as an internal reference for ^1H (δ = 7.23 ppm) and 85% H_3PO_4 in H_2O as an external standard for ^{31}P. Mass spectra were measured on Finnigan Mat TSQ 700 ESI.

Syntheses

All operations were performed in dinitrogen or argon atmosphere using standard Schlenk technique. Complexes $[Rh_2(\mu\text{-}OAc)_4(H_2O)_2]$ ([**1**·$(H_2O)_2$]) (43), $[Rh_2(\mu\text{-}OAc)_3\{\mu\text{-}(C_6H_3\text{-}4\text{-}OMe)P(C_6H_4O\text{-}4\text{-}OMe)_2\}(HOAc)_2]$ ([**4**·$(HOAc)_2$]) (21), $[Rh_2(\mu\text{-}OAc)_2\{\mu\text{-}(C_6H_3\text{-}4\text{-}OMe)P(C_6H_4\text{-}4\text{-}OMe)_2\}_2(HOAc)_2]$ ([**5**·$(HOAc)_2$]) (21), $[Rh_2(\mu\text{-}OAc)_3\{\mu\text{-}(C_6H_4\text{-}2\text{-}O)P(C_6H_4\text{-}2\text{-}OMe)_2\}(HOAc)]$ ([**6**·(HOAc)]) (19), and $[Rh_2(\mu\text{-}OAc)_3\{\mu\text{-}(C_6H_3\text{-}6\text{-}OMe\text{-}2\text{-}O)P[(C_6H_3\text{-}2,6\text{-}(OMe)_2]_2\}(HOAc)]$ ([**7**·(HOAc)]) (20) were synthesized according to literature methods.

[Rh_2(μ-OAc)$_2${μ-(C_6H_3-3-OMe)P(C_6H_4-3-OMe)$_2$}$_2$(HOAc)$_2$] ([3·(HOAc)$_2$])

A suspension of [**1**·$(H_2O)_2$] (0.144 g, 0.3 mmol) and MMP (0.226 g, 0.6 mmol) in a mixture of 5 cm^3 of ethanol and 5 cm^3 of acetic acid was refluxed with stirring for 3 h. The initial orange color of the reaction mixture was replaced by brown-gray and then by deep violet solution. The solution was evaporated to dryness and the product was crystallized from mixture of chloroform (5 cm^3) and acetic acid (3 cm^3). Yield: 0.316 g, 69%. Mass spectrum (M = $Rh_2(\mu\text{-}OAc)_2\{\mu\text{-}(C_6H_3\text{-}3\text{-}OMe)P(C_6H_4\text{-}3\text{-}OMe)_2\}_2$) (signals of intensity higher than 16%): 367 (100%) ($MMP^+ + CH_3$), 926 (18%), 967 (30%) ($M^+ - OAc$), 1335 (20%) ($M^+ - OAc + MMP + CH_3$), 1993 (20%) ($M_2^+ - OAc$). Anal. calcd. for $C_{50}H_{54}O_{14}P_2Rh_2$: C 52.37, H 4.75; found: C 52.42, H 4.71.

Fig. 3. UV–vis spectra of the mixtures of [**6**·(HOAc)] with adenine, adenosine, AMP, and ATP (in molar ratios 1:10) in the mixture of H_2O and AcMe (1:1 by volume). *X* axis: λ (nm), *Y* axis: $e = Ac_0^{-1}\ L^{-1}$.

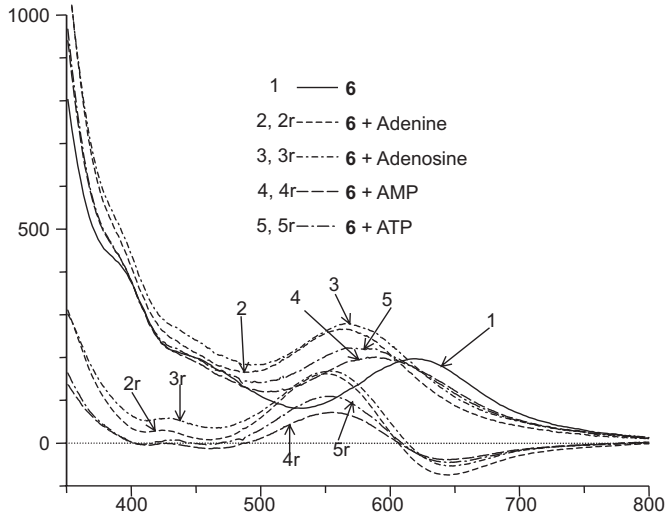

(η^5-C_5H_5)Fe(η^5-C_5H_4)$CH_2P(CH_2OH)_2$ (dhfmp) and {(η^5-C_5H_5)Fe(η^5-C_5H_4)CH_2}$_2PCH_2OH$ (hfmp)

Both phosphines were synthesized according to literature methods (44, 45) describing the synthesis of dhfmp as a single product.

19.27 g of an 80% solution of $P(CH_2OH)_4Cl$ in H_2O was diluted with MeOH (20 cm^3), deoxidized, and placed under an Ar atmosphere; KOH (4.26 g, 0.076 mol) was added to the solution. The resulting mixture was stirred for 2 h at room temperature. Then $[C_5H_5FeC_5H_4CH_2N(CH_3)_3]I$ (10.0 g, 0.026 mol) suspension in methanol (20 cm^3) was slowly added and the reaction mixture was refluxed with stirring for 20 h. After that time two-thirds of the solvent was evaporated and H_2O (15 cm^3), diethyl ether (45 cm^3), and triethylamine (15 cm^3) were added. After 1 h of stirring, the water layer was removed and reextracted with diethyl ether (15 cm^3). The combined extracts were washed a few times with small portions (5 cm^3) of water (to dispel the characteristic smell of amine). After removing ether under reduced pressure, the products were recrystallized from the mixture of CH_2Cl_2 (5 cm^3), MeOH (5 cm^3), and light petroleum ether (35 cm^3). In all experiments, we have always obtained two products, which were isolated using the difference of their solubility in the mixture of water and methanol. In methanol–water (50:50 by mass) practically only dhfmp is dissolved. The purity of products was controlled using TLC (5 × 20 cm plates with reversed phase silicagel (C_{18}) from Alltech). Eluent: 90% solution of methanol in water. Intense yellow color of products facilitated the

Table 7. ID_{50} [μg mL^{-1}] ([mol dm^{-3}]).

	KB (oral carcinoma)	Hu1703 (bladder cancer)	SW707 (colon adenocarcinoma)	T47D (breast cancer)
[**6**·(HOAc)]	9.12 ± 2.00 (1.17×10^{-6})	0.309 ± 0.0013 (3.96×10^{-7})	0.427 ± 0.0012 (5.47×10^{-7})	0.302 ± 0.0012 (3.87×10^{-7})
[**7**·(HOAc)]	55.00 ± 1.90 (6.32×10^{-5})	5.100 ± 0.013 (5.86×10^{-6})	38.000 ± 0.001 (4.36×10^{-5})	3.550 ± 0.001 (4.08×10^{-6})
[**3**·$(HOAc)_2$]	66.00 ± 1.80 (5.76×10^{-5})	46.000 ± 0.001 (4.01×10^{-5})	49.000 ± 0.001 (4.27×10^{-5})	38.000 ± 0.001 (3.31×10^{-5})
dhfmp	74.0 ± 0.00 (2.53×10^{-4})	39.000 ± 0.001 (1.34×10^{-4})	40.000 ± 0.001 (1.37×10^{-4})	45.000 ± 0.001 (1.54×10^{-4})
$Pt(NH_3)_2Cl_2$ (*cis*-platin)	—	0.23 (7.66×10^{-7})	3.0 (1.00×10^{-5})	—

Fig. 4. UV–vis spectra of the mixtures of [**6**·(HOAc)] with GSH, GSSG, and cysteine (in molar ratios given in the figure) in the mixture of H_2O and AcMe (1:1 by volume). *X* axis: λ (nm), *Y* axis: $e = Ac_0^{-1}\ L^{-1}$.

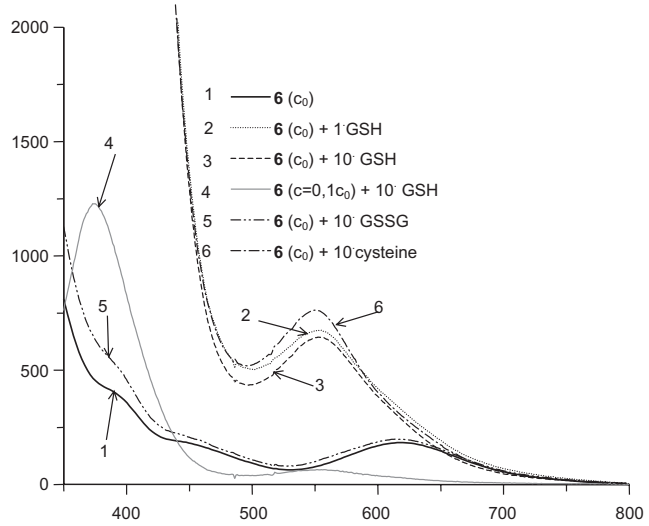

Fig. 5. UV–vis spectra of the mixtures of [**3**·$(HOAc)_2$] with GSH and cysteine (in molar ratios given in the figure) in the mixture of H_2O and AcMe (1:1.5 by volume). *X* axis: λ (nm), *Y* axis: $e = Ac_0^{-1}\ L^{-1}$.

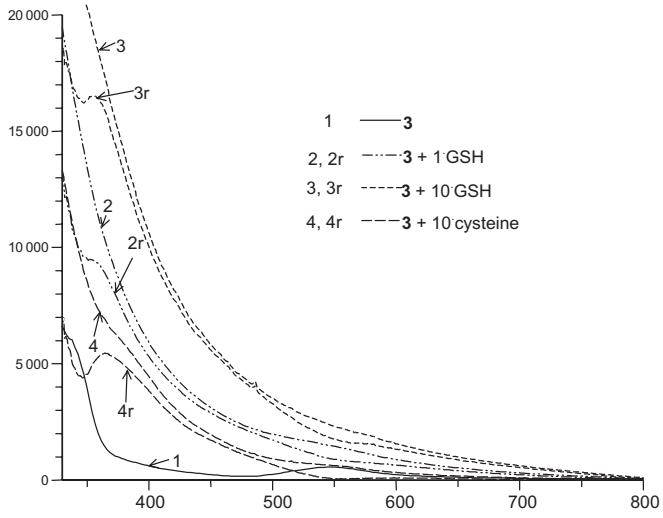

observations. Yield: 47% for dhfmp and 21% for hfmp. Mass spectrum of dhfmp (M = $(C_5H_5)Fe(C_5H_4)CH_2P(CH_2OH)_2$) (signals of intensity higher than 16%): 199 (100%) $\{FcCH_2^+\}$, 292 (20%) $\{M^+\}$, 322 (42%) $\{M^+ + CH_2OH\}$, 460 (18%) $\{(FcCH_2)_2P(CH_2OH)^+\}$, 490 (20%) $\{(FcCH_2)_2PH(CH_2OH)_2\}$. Mass spectrum of hfmp (M = $\{(C_5H_5)Fe(C_5H_4)CH_2\}_2PCH_2OH$) (signals of intensity higher than 16%): 199 (72%) $\{FcCH_2^+\}$, 461 (100%) $\{M^+ + H\}$, 491 (68%) $\{M^+ + CH_2OH\}$. Anal. calcd. for $C_{13}H_{17}FeO_2P$ (dhfmp): C 53.46, H 5.87, P 10.60; found: C 53.4, H 5.6, P 9.8. Anal. calcd. for $C_{23}H_{25}Fe_2OP$ (hfmp): C 60.04, H 5.48, P 6.73; found: C 59.8, H 5.3, P 6.4.

X-ray structure determination

All measurements were made at 170(2) K on a Kuma KM4CCD κ-axis diffractometer with graphite monochromated Mo Kα radiation (λ = 0.71073 Å, 3.30 = θ = 27.00). The crystallographic data together with data collection and structure refinement details are given in Table 2. All the data were corrected for Lorentz and polarization effects but absorption and extinction were not applied. The crystal was positioned at 65 mm from the KM4CCD camera. Frames (612) were measured at 0.75° intervals with a counting time of 20 s. The data were corrected for Lorentz and polarization effects. Data reduction and analysis were carried out with the Kuma Diffraction programs (46, 47). The structure was solved by direct methods and refined by the full-matrix least-squares method on F^2 (48). The refinement was performed using the SHELXL program (49). Non-hydrogen atoms were refined with anisotropic thermal parameters; hydrogen atoms were included from the geometry of molecules and Δρ maps but were not refined.

Crystals of [**3**·(HOAc)(H_2O)] suitable for X-ray analysis were obtained from recrystallization of [**3**·$(HOAc)_2$] from the mixture of $CHCl_3$ and 96% EtOH in H_2O.

Cytotoxic activity in vitro

Compounds

Test solutions of the compounds tested (1 mg mL^{-1}) were prepared ex tempore by dissolving the substance in 100 μL of solvent completed with 900 μL of tissue culture medium. Afterwards, the tested compounds were diluted in culture medium (described below) to reach the final concentrations of 100, 10, 1, 0.1, and 0.01 μg mL^{-1}. The solvents (in dilu-

tion corresponding to its highest concentration applied to the tested compounds), did not exert any inhibitory effect on cell proliferation.

Cells

The below listed, established in vitro, human cancer cell lines were applied: SW707 (colon adenocarcinoma), Hu1703 (bladder cancer), T47D (breast cancer), KB (oral carcinoma). All lines were obtained from the American Type Culture Collection (Rockville, Maryland, U.S.A.) and are maintained in the Cell Culture Collection of the Institute of Immunology and Experimental Therapy, Wroclaw, Poland.

The cells were plated in 96-well plates (Sarstedt, U.S.A.) at a density of 1×10^4 cells per well, 24 h before addition of the tested agents. The cells were cultured in the opti-MEM medium supplemented with 2mM glutamine (Gibco, Warsaw, Poland), streptomycin (50 μg mL^{-1}), penicillin (50 U mL^{-1}) (both antibiotics from Polfa, Tarchomin, Poland), and 5% fetal calf serum (Gibco, Grand Island, New York). The cell cultures were maintained at 37°C in a humid atmosphere saturated with 5% CO_2.

Antiproliferative assay in vitro

SRB. The details of this technique were described by Skehan et al. (50). The cytotoxicity assay was performed after 72-h exposure of the cultured cells to varying concentrations (from 0.01 to 100 μg mL^{-1}) of the tested agents. The cells attached to the plastic were fixed by gently layering cold 50% TCA (trichloroacetic acid, Aldrich-Chemie, Germany) on the top of the culture medium in each well. The plates were incubated at 4°C for 1 h and then washed five times with tap water. The background optical density was measured in the wells filled with culture medium, without the cells. The cellular material fixed with TCA was stained with 0.4% sulforhodamine B (SRB, Sigma, Germany) dissolved in 1% acetic acid (POCh, Gliwice, Poland) for 30 min. Unbound dye was removed by rinsing (4×) with 1% acetic acid. The protein-bound dye was extracted with 10 mM unbuffered Tris base (tris (hydroksymethyl) aminomethane, POCh, Gliwice, Poland) for determination of optical density (at 540 nm) in a computer-interfaced, 96-well microtiter plate reader Multiskan RC photometer (Labsystems). Each compound in given concentration was tested in triplicates in each experiment, which was repeated 3–5 times.

The results of cytotoxic activity in vitro were expressed as ID_{50} — the dose of compound that inhibits proliferation rate of the tumor cells by 50% as compared to control untreated cells.

Supplementary material

Supplementary material may be purchased from the Depository of Unpublished Data, Document Delivery, CISTI, National Research Council Canada, Ottawa, ON K1A 0S2, Canada (for information on ordering electronically http://www.nrc.ca/cisti/irm/unpub_e.shtml). Crystallographic data (excluding structure factors) for the structure reported in this paper have been deposited with the Cambridge Crystallographic Data Centre. Copies of the data can be obtained, free of charge, on application to the Director, CCDC, 12 Union Road, Cambridge CB2, 1EZ, U.K. (Fax: (+44)1223-336-033 or e-mail: deposit@ccdc.cam.ac.uk).

References

1. A.R. Chakravarty, F.A. Cotton, D.A. Tocher, and J.H. Tocher. Organometallics, **4**, 8 (1985).
2. F.A. Cotton, F. Barcelo, P. Lahuerta, R. Llusar, J. Paya, and M.A. Ubeda. Inorg. Chem. **27**, 1010 (1988).
3. P. Lahuerta, J. Paya, E. Peris. M.A. Pellinghelli, and A. Tiripicchio. J. Organomet. Chem. **373**, C5 (1989).
4. M.V. Borrachero, F. Estevan, S. Garcia-Granda, P. Lahuerta, J. Latorre, E. Peris, and M. Sanau. J. Chem. Soc. Chem. Comm. 1864 (1993).
5. P. Lahuerta, J. Paya, X. Solans, and M.A. Ubeda. Inorg. Chem. **31**, 385 (1992).
6. P. Lahuerta, J. Paya, E. Peris, A. Aguirre, S. Garcia-Granda, and F. Gomez-Beltran. Inorg. Chim. Acta, **192**, 43 (1992).
7. P. Lahuerta, J. Paya, M.A. Pellinghelli, and A. Tiripicchio. Inorg. Chem. **31**, 1224 (1992).
8. A. Garcia-Bernabe, P. Lahuerta, M.A. Ubeda, S. Garcia-Granda, and P. Pertierra. Inorg. Chim. Acta, **229**, 203 (1995).
9. F. Estevan, S. Garcia-Granda, P. Lahuerta, J. Latorre, E. Peris, and M. Sanau. Inorg. Chim. Acta, **229**, 365 (1995).
10. P. Lahuerta, J. Paya, S. Garcia-Granda, F. Gomez-Beltran, and A. Anillo. J. Organomet. Chem. **443**, C14 (1993).
11. S. Garcia-Granda, P. Lahuerta, J. Latorre, M. Martinez, E. Peris, M. Sanau, and M.A. Ubeda. J. Chem. Soc. Dalton Trans. 539 (1994).
12. G. Gonzalez, M. Martinez, F. Estevan, A. Garcia-Bernabe, P. Lahuerta, E. Peris, M.A. Ubeda, M.R. Diaz, S. Garcia-Granda, and B. Tejerina. New J. Chem. **20**, 83 (1996).
13. G. Gonzalez, P. Lahuerta, M. Martinez, E. Peris, and M. Sanau. J. Chem. Soc. Dalton Trans. 545 (1994).
14. F. Estevan, G. Gonzalez, P. Lahuerta, M. Martinez, E. Peris, and R. van Eldik. J. Chem. Soc. Dalton Trans. 1045 (1996).
15. F.P. Pruchnik, R. Starosta, P. Smolenski, E. Shestakova, and P. Lahuerta. Organometallics, **17**, 1395 (1998).
16. S.J. Chen and K.R. Dunbar. Inorg. Chem. **29**, 588 (1990).
17. S.J. Chen and K.R. Dunbar. Inorg. Chem. **30**, 2018 (1991).
18. K.R. Dunbar, J.H. Matonic, and V.P. Saharan. Inorg. Chem. **33**, 25 (1994).
19. Z. Galdecki, E. Galdecka, A. Kowalski, F.P. Pruchnik, K. Wajda-Hermanowicz, and R. Starosta. Pol. J. Chem. **73**, 859 (1999).
20. F.P. Pruchnik, R. Starosta, M.W. Kowalska, E. Galdecka, Z. Galdecki, and A. Kowalski. J. Organomet. Chem. **597**, 20 (2000).
21. R.G. Hughes, J.L. Bear, and A.P. Kimball. Proc. Am. Assoc. Cancer Res. **13**, 120 (1972).
22. F.A. Cotton and R.A. Walton. Multiple bonds between metal atoms. Clarendon Press, Oxford. 1993.
23. E.B. Boyar and S.D. Robinson. Coord. Chem. Rev. **50**, 109 (1983).
24. N. Farrel and M.P. Hacker. Inorg. Chim. Acta, **166**, 35 (1989).
25. F.P. Pruchnik and D. Dus. J. Inorg. Biochemistry, **61**, 55 (1996).
26. F.P. Pruchnik, M. Bien, and T. Lachowicz. Met. Based Drugs, **3**, 185 (1996).
27. M. Bien, T.M. Lachowicz, A. Rybka, F.P. Pruchnik, and L. Trynda. Met. Based Drugs, **4**, 81 (1997).
28. M. Bien, F.P. Pruchnik, A. Seniuk, T.M. Lachowicz, and P. Jakimowicz. J. Inorg. Biochem. **73**, 49 (1999).
29. L. Trynda and F.P. Pruchnik. J. Inorg. Biochem. **58**, 69 (1995).

30. L. Trynda-Lemiesz and F.P. Pruchnik. J. Inorg. Biochem. **66**, 187 (1997).
31. F.P. Pruchnik, G. Kluczewska, A. Wilczok, U. Mazurek, and T. Wilczok. J. Inorg. Biochem. **65**, 25 (1997).
32. F.P. Pruchnik, R. Starosta, T. Lis, and P. Lahuerta. J. Organomet. Chem. **568**, 177 (1998).
33. N. Farrell. J. Inorg. Biochem. **14**, 261 (1981).
34. N. Alberding, N. Farrell, and E.D. Crozier. J. Am. Chem. Soc. **107**, 384 (1985).
35. J.R. Rubin, T.P. Haromy, and M. Sundaralingam. Acta Crystallogr. Sect. C: Cryst. Struct. Commun. **47**, 1712 (1991).
36. P. Jakimowicz, L. Ostropolska, and F.P. Pruchnik. Met. Based Drugs, **7**, 201 (2000).
37. V.M. Miskowski, I.S. Sigal, K.R. Mann, H.B. Gray, S.J. Milder, G.S. Hammond, and P.R. Ryason. J. Am. Chem. Soc. **101**, 4383 (1979).
38. V.M. Miskowski, G.L. Nobinger, D.S. Kliger, G.S. Hammond, N.S. Lewis, K.R. Mann, and H.B. Gray. J. Am. Chem. Soc. **100**, 485 (1978).
39. I.S. Sigal and H.B. Gray. J. Am. Chem. Soc. **103**, 2220 (1981).
40. N.S. Lewis, K.R. Mann, J.G. Gordon II, and H.B. Gray. J. Am. Chem. Soc. **98**, 7461 (1976).
41. E. Galdecka, Z Galdecki, F.P. Pruchnik, and P. Jakimowicz. Transition Met. Chem. (Dordrecht, Neth.), **25**, 315 (2000).
42. F.P. Pruchnik, P. Jakimowicz, Z. Ciunik, K. Stanislawek, L. Oro, C. Tejel, and M.A. Ciriano. Inorg. Chem. Comm. **4**, 19 (2001).
43. G.L. Rempel, P. Legzdins, H. Smith, and G. Wilkinson. Inorg. Synth. **13**, 90 (1972).
44. N.J. Goodwin, W. Henderson, and J.K. Sarfo. J. Chem. Soc. Chem. Comm. 1551 (1996).
45. N.J. Goodwin, W. Henderson, and B.K. Nicholson. J. Chem. Soc. Chem. Comm. 31 (1997).
46. KM4RED data reduction program. Kuma Diffraction Ltd., Wroclaw, Poland. 1997.
47. KM4CCD data collection program. Kuma Diffraction Ltd., Wroclaw, Poland. 1997.
48. G.M. Sheldrick. SHELXS 97. Program for the solution of crystal structures. University of Göttingen, Germany. 1997.
49. G.M. Sheldrick. SHELXL 97. Program for the refinement of crystal structures. University of Göttingen, Germany. 1997.
50. P. Skehan, R. Storeng, D. Scudiero, et al. J. Nat. Cancer Inst. **82**, 1107 (1990).